Ubiquitin-dependent lysosomal targeting of $GABA_A$ receptors regulates neuronal inhibition

I. Lorena Arancibia-Cárcamo[a], Eunice Y. Yuen[b], James Muir[a], Michael J. Lumb[a], Guido Michels[c], Richard S. Saliba[d], Trevor G. Smart[a], Zhen Yan[b], Josef T. Kittler[a,1,2], and Stephen J. Moss[a,d,1,2]

[a]Department of Neuroscience, Physiology, and Pharmacology, University College London, Gower Street, London, WC1E 6BT, United Kingdom; [b]Department of Physiology and Biophysics, State University of New York, Buffalo, NY 14214; [c]Department of Internal Medicine, University of Cologne, 50937 Cologne, Germany; and [d]Department of Neuroscience, Tufts University School of Medicine, 136 Harrison Avenue Boston, MA 02111

Edited by Richard L. Huganir, Johns Hopkins University School of Medicine, Baltimore, MD, and approved August 31, 2009 (received for review May 19, 2009)

The strength of synaptic inhibition depends partly on the number of $GABA_A$ receptors ($GABA_A$Rs) found at synaptic sites. The trafficking of $GABA_A$Rs within the endocytic pathway is a key determinant of surface $GABA_A$R number and is altered in neuropathologies, such as cerebral ischemia. However, the molecular mechanisms and signaling pathways that regulate this trafficking are poorly understood. Here, we report the subunit specific lysosomal targeting of synaptic $GABA_A$Rs. We demonstrate that the targeting of synaptic $GABA_A$Rs into the degradation pathway is facilitated by ubiquitination of a motif within the intracellular domain of the γ2 subunit. Blockade of lysosomal activity or disruption of the trafficking of ubiquitinated cargo to lysosomes specifically increases the efficacy of synaptic inhibition without altering excitatory currents. Moreover, mutation of the ubiquitination site within the γ2 subunit retards the lysosomal targeting of $GABA_A$Rs and is sufficient to block the loss of synaptic $GABA_A$Rs after anoxic insult. Together, our results establish a previously unknown mechanism for influencing inhibitory transmission under normal and pathological conditions.

endocytosis | trafficking | ischemia | ion channels | synapse

The strength of inhibitory synapses is a major determinant of neuronal processing and excitability and can be determined by the number of γ-amino butyric acid type A receptors ($GABA_A$Rs) found at synaptic sites (1–3). Moreover, in a number of neuropathologies, including status epilepticus and in vitro and in vivo models of cerebral ischemia, the rapid down-modulation of synaptic $GABA_A$Rs has been reported to contribute to pathological disinhibition, excitotoxicity, and cell death (4–8). However, the molecular mechanisms and signaling pathways that regulate $GABA_A$R trafficking, under normal or pathological conditions, remain unclear.

$GABA_A$Rs undergo significant rates of endocytosis, a process that can rapidly modify receptor number at synapses (9). Upon internalization, receptors are either reinserted into the plasma membrane or targeted for degradation (10). The balance between these two processes is critical for determining the number of receptors expressed at synapses and hence neuronal excitability (11). However, the regulatory mechanisms that control this endocytic sorting of synaptic $GABA_A$Rs remain unknown.

The trafficking of membrane proteins can be regulated via the covalent attachment of the 76 amino acid (aa) peptide, ubiquitin, or ubiquitin-like proteins to lysine residues within target proteins (12, 13). A number of studies on the role of ubiquitination in regulating synaptic function under normal conditions and in pathological conditions such as ischemia have focused on the ubiquitin-proteasome system (14–18). However, within the endocytic pathway, mono-ubiquitination (or the addition of short ubiquitin chains) is a key signal that results in the specific targeting of cargo to late endosomes for subsequent lysosomal degradation (12, 19, 20). The significance of ubiquitination in determining the endocytic fate and degradation of neurotransmitter receptors remains to be established.

In the present study we investigated the role of $GABA_A$R ubiquitination in regulating $GABA_A$R endosomal trafficking. We show that the $GABA_A$R γ2 subunit, which plays a key role in synaptic targeting, can preferentially target internalized $GABA_A$Rs to the lysosome for degradation. We demonstrate that this process is regulated by an amino acid motif within the intracellular loop of the γ2 subunit, which is a target for ubiquitination and that mutation of this motif retards the lysosomal targeting of $GABA_A$Rs. Inhibition of lysosomal activity or the trafficking of ubiquitinated proteins to lysosomal compartments increases the accumulation of $GABA_A$Rs at synapses and the efficacy of synaptic inhibition. Furthermore, we demonstrate that the loss of surface $GABA_A$Rs observed in an in vitro model of ischemia can be inhibited by blocking ubiquitination of the lysosomal targeting motif in the γ2 subunit. Thus, our results demonstrate that $GABA_A$R ubiquitination is a key mechanism for regulating the strength and plasticity of synapses and the efficacy of neuronal inhibition under both normal and pathological conditions.

Results

Lysosomal Activity Regulates the Accumulation of Synaptic $GABA_A$Rs and the Inhibitory Synaptic Response. We initially investigated whether the extent of lysosomal $GABA_A$R degradation is a functionally relevant mechanism for regulating the size and number of postsynaptic $GABA_A$Rs and hence the strength of synaptic inhibition. For this, acute coronal cortical slices from P21 rats were treated with the lysosomal protease inhibitor leupeptin (200 μM, 3 h). Slices were fixed and stained with antibodies against $GABA_A$Rs and the inhibitory presynaptic marker VIAAT (21) and imaged using confocal microscopy (Fig. 1 *A* and *B*). Leupeptin treatment resulted in an increase in the mean postsynaptic $GABA_A$R cluster size (Ctrl: 0.45 ± 0.04 μm^2; Leu: 0.63 ± 0.02 μm^2) revealed by a rightward shift in the cumulative cluster area distributions (Fig. 1 *C* and *D*). In addition, we found a significant increase in the number of synaptic GABAergic clusters per cell (Ctrl: 15.2 ± 1.2; Leu: 27.3 ± 2.4) (Fig. 1*E*). In contrast, clusters that were not found to have a presynaptic counterpart were unaltered in size (Ctrl: 0.40 ± 0.05 μm^2; Leu: 0.45 ± 0.04 μm^2) or number (Ctrl: 3.8 ± 0.7; Leu: 3.8 ± 0.9).

To assess whether this increase in the $GABA_A$R cluster size and number resulted in modified synaptic inhibition, we compared the properties of miniature or evoked inhibitory postsynaptic currents

Author contributions: I.L.A.-C., E.Y.Y., Z.Y., J.T.K., and S.J.M. designed research; I.L.A.-C., E.Y.Y., J.M., and G.M. performed research; I.L.A.-C., M.J.L., and R.S.S. contributed new reagents/analytic tools; I.L.A.-C., E.Y.Y., J.M., G.M., and Z.Y. analyzed data; and I.L.A.-C., T.G.S., J.T.K., and S.J.M. wrote the paper.

The authors declare no conflict of interest.

This article is a PNAS Direct Submission.

[1]J.T.K. and S.J.M. contributed equally to this work.

[2]To whom correspondence may be addressed. E-mail: j.kittler@ucl.ac.uk or stephen.moss@tufts.edu.

This article contains supporting information online at www.pnas.org/cgi/content/full/0905502106/DCSupplemental.

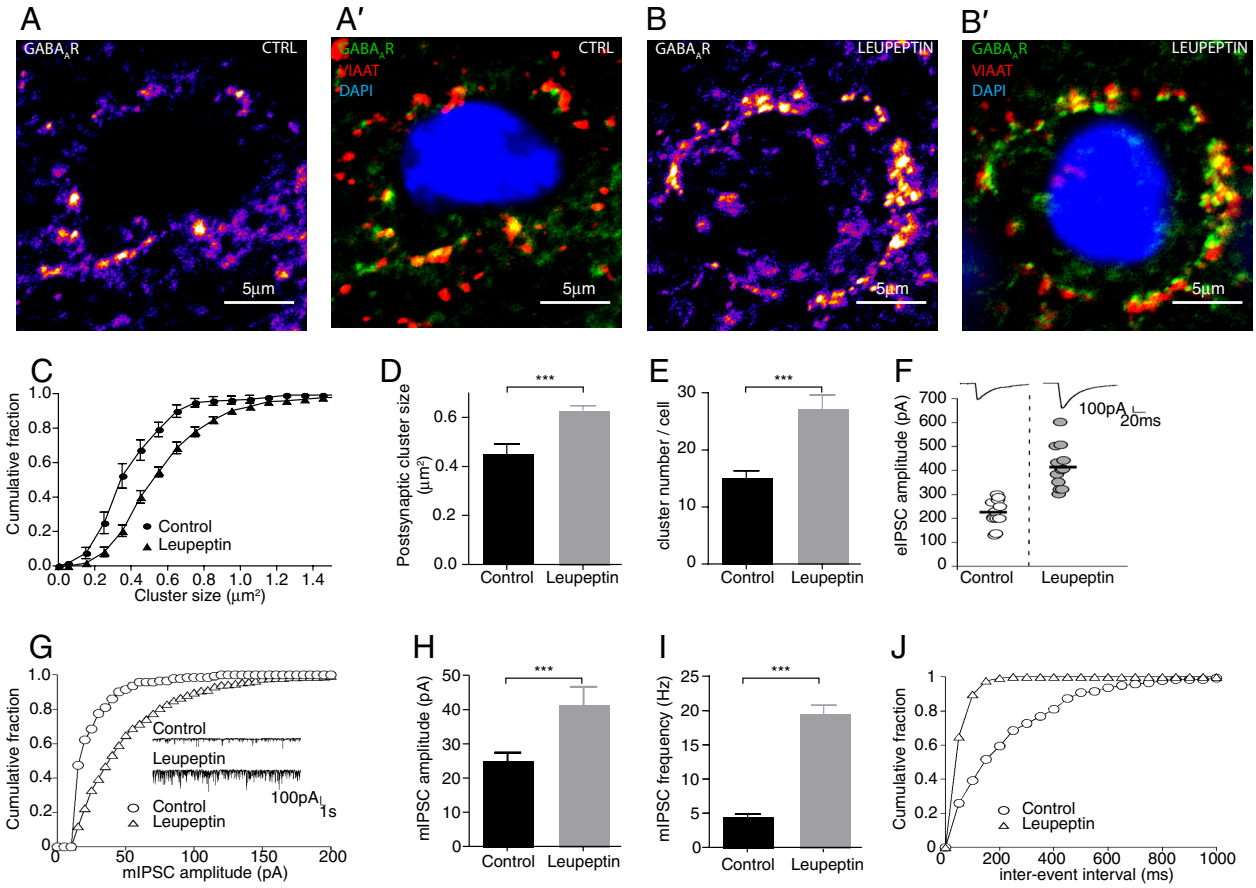

Fig. 1. Functional effects of disrupting lysosomal degradation (*A–E*) GABA$_A$R cluster analysis on control and leupeptin treated cortical slices. High resolution confocal images were taken of 25-μm sections across the cells bodies (identified by DAPI nuclear staining, blue). (*A* and *B*) Pseudocolor images of GABA$_A$R clusters. Clusters can be identified by changes in intensity (blue to pink to white) over a central point. (*A′* and *B′*) Merged images show GABA$_A$R clusters (green) apposed to presynaptic VIAAT positive terminals (red). (*C*) Cumulative plot showing the cluster size distributions under control and leupeptin treated conditions. (*D*) Average GABA$_A$R cluster size in control and leupeptin treated cells. (*E*) Average number of GABA$_A$R clusters in control and leupeptin treated cells (n = 11–12 cells; ***, $P < 0.001$). (*F*) Summary data plot of the effect of leupeptin on eIPSC density (n = 12, $P < 0.001$ unpaired t test). (*G*) Representative cumulative plots and traces (*Inset*) of mIPSC amplitude for representative cells from cortical slices under control and leupeptin treated conditions. (*H*) Bar plot summary showing the effect of leupeptin on mIPSC amplitude (n = 7, ***, $P < 0.001$). (*I*) Bar plot summary showing the effect of leupeptin on mIPSC frequency (n = 7, ***, $P <$ 0.001). (*J*) Representative cumulative plots of mIPSC inter-event interval of representative cells under control and leupeptin treated conditions.

(mIPSCs or eIPSCs) between control neurons and those treated with leupeptin using whole cell recording. In agreement with our labeling data, leupeptin treatment resulted in a significant increase in the eIPSC current amplitude (Ctrl: 223.6 ± 16 pA; Leu: 412.5 ± 26 pA) (Fig. 1*F*). In addition, leupeptin treatment caused a sustained increase in mIPSC amplitude (41.6 ± 5.1pA) compared with untreated control cells (25.3 ± 2.2 pA) (Fig. 1 *G* and *H*) revealed by the rightward shift in the cumulative amplitude relationship for mIPSCs. Leupeptin treatment also caused a significant enhancement in mIPSC frequency (Ctrl: 4.6 ± 0.3 Hz; Leu: 19.6 ± 1.2 Hz) (Fig. 1 *I* and *J*). However, leupeptin did not alter mIPSC kinetics (Table S1). In contrast, the mean amplitudes (Ctrl: 7.5 ± 0.6 pA; Leu: 8.9 ± 0.6 pA) and frequency (Ctrl: 2.5 ± 0.19 Hz; Leu: 2.7 ± 0.18 Hz) of miniature excitatory postsynaptic currents (mEPSC) or the eEPSC current amplitude (Ctrl: 108.8 ± 7.7 pA; Leu: 118 ± 8.9 pA) were unaffected by leupeptin treatment (Fig. S1). Thus, blockade of lysosomal GABA$_A$R degradation results in an increase in the number and size of synaptic GABA$_A$R clusters leading to increased synaptic inhibition.

Identification of a Sorting Motif in the GABA$_A$R γ2 Subunit That Facilitates Lysosomal Targeting of GABA$_A$Rs. Having established that lysosomal degradation of GABA$_A$Rs is an important determinant of the number of surface and synaptic GABA$_A$Rs, we next set out to identify the molecular mechanisms that mediate lysosomal targeting of GABA$_A$Rs. Because the γ2 subunit is an important determinant for the trafficking of GABA$_A$Rs, and their entry into the endocytic pathway (22–25), we examined the possible role that this subunit plays in receptor lysosomal targeting. We compared the lysosomal targeting in HEK-293 cells of GABA$_A$Rs composed of $\alpha\beta$ and $\alpha\beta\gamma2$ subunits modified with N-terminal 9E10 reporters. To identify late endocytic/lysosomal compartments we coexpressed GABA$_A$Rs with GFP-Rab7, a marker for late endosomal and lysosomal structures (26, 27). To specifically label receptors in the endocytic pathway, live cells were labeled with myc antibody for 30 min at 4 °C and then placed at 37 °C to allow for internalization. After fixation and permeabilization, internalized receptors were visualized and their distribution in confocal slices showing maximum receptor internalization was compared with that for GFP-Rab7. Endocytosed $\alpha\beta\gamma2$ receptors exhibited a marked increase in targeting to late endosomes/lysosomes as demonstrated by a substantially increased colocalization with GFP-Rab7 compared with those composed of $\alpha\beta$ subunits ($\alpha\beta$: 43.3 ± 4.1%; $\alpha\beta\gamma2$: 67.8 ± 5.2%) (Fig. 2 *A–C*). This suggests a significant role for the γ2 subunit in regulating the targeting of GABA$_A$Rs to the late endosomal/lysosomal compartments.

To identify the domain of the γ2 subunit that mediates the lysosomal targeting of GABA$_A$Rs we exploited the ability of

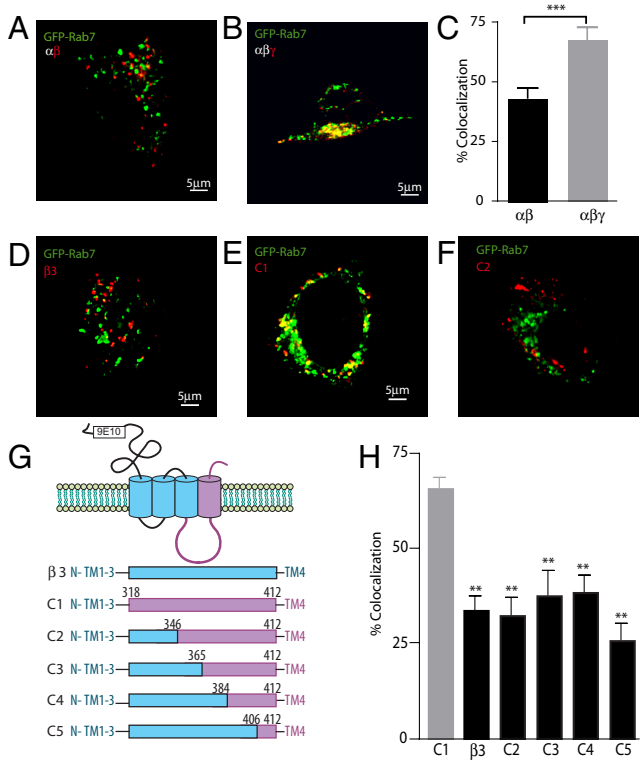

Fig. 2. γ2 subunit dependent lysosomal targeting of $GABA_A$Rs. (*A* and *B*) Representative images of internalized $GABA_A$Rs (red) comprised of α1β3 (*A*) or α1β3γ2 (*B*) in HEK293 cells coexpressed with the late endosomal/lysosomal marker GFP-Rab7 (green). Areas of overlap are seen in yellow. (*C*) Summary data of the colocalization levels between internalized $GABA_A$Rs and GFP-Rab7 (n = 14–16, ***, $P < 0.001$). (*D–F*) Representative images of internalized β3 subunits or β3-γ2 chimeras C1–C2 (red) in HEK293 cells coexpressed with the late endosomal/lysosomal marker GFP-Rab7 (green). Areas of overlap are seen in yellow. (*G*) Schematic diagram of β3-γ2 chimeras C1–C5. (*H*) Summary data of the percent colocalization levels of internalized C1–C5 and GFP-Rab7 (n = 8–12, **, $P < 0.01$).

$GABA_A$R β3 subunits to assemble into pentameric cell surface homomeric ion channels, a property that depends on residues within the N terminus of this subunit (28, 29). As measured by antibody labeling, internalized β3 subunits showed a similar distribution to αβ receptors with respect to GFP-Rab7 (33.8 ± 3.7%) (Fig. 2 *D* and *H*). In contrast, a chimeric receptor (C1) in which the major intracellular domain and transmembrane domain 4 of the β3 subunit were exchanged for the corresponding domains of the γ2 subunit (Fig. 2*G*) exhibited enhanced targeting to lysosomes, as measured by colocalization with GFP-Rab7 similar to levels seen with αβγ2 subunit containing receptors (63.3 ± 3.6%) (Fig. 2 *E* and *H*). Thus, the intracellular domain and/or TM4 of the γ2 subunit are sufficient to mediate the lysosomal targeting of $GABA_A$Rs.

To identify the region within the γ2 subunit responsible for the late endosomal/lysosomal targeting of $GABA_A$Rs, we constructed a set of β3/γ2 subunit chimeras that serially replaced sequences within C1 with those from the β3 subunit (Fig. 2*G*). Using live cell antibody labeling experiments we followed the extent of lysosomal targeting of internalized β3/γ2 chimeras by their colocalization with GFP-Rab7. Compared with C1, chimeras C2, C3, C4, and C5 all showed reduced levels of colocalization with GFP-Rab7 (71.7 ± 3.4% compared with 31.8 ± 2.5%, 37.7 ± 6.4%, 38.6 ± 4.4%, 25.9 ± 4.3%, respectively) (Fig. 2 *E*, *F*, and *H*, and Fig. S2). Thus, residues 318–337 in the γ2-subunit intracellular domain, proximal to TM3 contain the late endosomal/lysosomal targeting sequence because replacement of this sequence with that of β3 abrogated the enhanced colocalization of the β3/γ2 chimeras with GFP-Rab7.

Blockade of Ubiquitin-Dependent Lysosomal Sorting Increases $GABA_A$R Functional Expression. Ubiquitination of lysine residues can act as a signal for sorting membrane proteins to the lysosome for degradation (12). We noted that residues 318–337 of the γ2 subunit contain a number of conserved lysine residues (Fig. S3), suggesting that the late endosomal/lysosomal targeting of γ2 subunit containing $GABA_A$Rs may be dependent on ubiquitination. The ubiquitin dependent sorting of membrane proteins to the lysosome depends on a highly conserved machinery that specifically recognizes ubiquitinated membrane proteins in the early endosome and selects them for late endosomal/lysosomal sorting (30). The hepatocyte growth factor regulated substrate (Hrs) is a key component of this initial recognition machinery and we took advantage of GFP-2FYVE, a dominant negative construct known to block the lysosomal targeting of ubiquitinated proteins by disrupting Hrs function (31). We first assessed the ability of this construct to modulate the trafficking of $GABA_A$Rs by assessing its effect on steady state surface levels of these receptors in transfected neurons. As measured by cell surface biotinylation, neurons transfected with GFP-2FYVE exhibited a 68.2 ± 11.1% increase in the cell surface expression levels of $GABA_A$Rs compared with those expressing GFP alone (Fig. 3 *A* and *B*).

We further investigated whether the increase in cell surface accumulation of $GABA_A$Rs in the presence of GFP-2FYVE alters the properties of mIPSCs using whole cell recording. Similar to our results using leupeptin, expression of GFP-2FYVE in cultured hippocampal neurons resulted in a 66.3% increase in the mean mIPSC amplitude compared with cells expressing GFP (GFP-2FYVE: 50.4 ± 2.4 pA, n = 9; GFP: 30.3 ± 1.2 pA, n = 8) (Fig. 3 *C* and *D*). In addition, expression of GFP-2FYVE also caused a significant enhancement in mIPSC frequency compared with control cultures expressing GFP alone (GFP-2FYVE: 7.9 ± 0.5 Hz, n = 9; GFP: 3.2 ± 0.6 Hz, n = 8) (Fig. 3 *C*, *E*, and *F*). As for leupeptin treatment, channel kinetics were unaffected by GFP-2FYVE expression (Table S2). These results demonstrate that ubiquitin-dependent targeting of $GABA_A$Rs to lysosomal compartments plays a key role in regulating the number of $GABA_A$Rs at synaptic sites together with the efficacy of neuronal inhibition.

Lysosomal Targeting of $GABA_A$Rs Is Regulated by Ubiquitination of the γ2 Subunit. Our results indicate that ubiquitination of $GABA_A$Rs within the endocytic pathway can determine the lysosomal degradation of $GABA_A$Rs and our mapping experiments suggested that the lysine residues within the γ2 subunit lysosomal targeting motif are likely to be the site of ubiquitination. To analyze this further, we compared the ubiquitination of $GABA_A$Rs containing WT γ2 subunits or a construct in which K325, K328, K330, K332, K333, K334, and K335 within the lysosomal targeting motif were all mutated to arginine residues ($\gamma2^{K7R}$). The ubiquitination of these constructs was tested in HEK cells expressing $\alpha1\beta3^{9E10}\gamma2$ (or $\alpha1\beta3^{9E10}\gamma2^{K7R}$) and HA-tagged ubiquitin. Cells were lysed, and the γ2 subunit was immunoprecipitated with anti-myc and immunoblotted with anti-HA and anti-9E10. This revealed significant levels of ubiquitination for the WT γ2 subunit, which was largely abolished for the $\gamma2^{K7R}$ construct despite similar levels of γ2 subunit immunoreactivity. Therefore, these experiments suggest that the principle sites of ubiquitination within the γ2 subunit intracellular domain lie between residues 325 and 335 (Fig. 4*D*).

We then tested the role of the respective lysine residues in facilitating sorting of αβγ2 receptors to the late endosome/lysosome. Live antibody labeling experiments showed that mutation of the lysine residues within the endocytic sorting motif did not alter receptor internalization (Fig. 4*B*). In contrast, receptors expressing $\gamma2^{K7R}$ exhibited reduced levels of late endosomal/lysosomal targeting compared with those expressing wild-type γ2, as assessed by

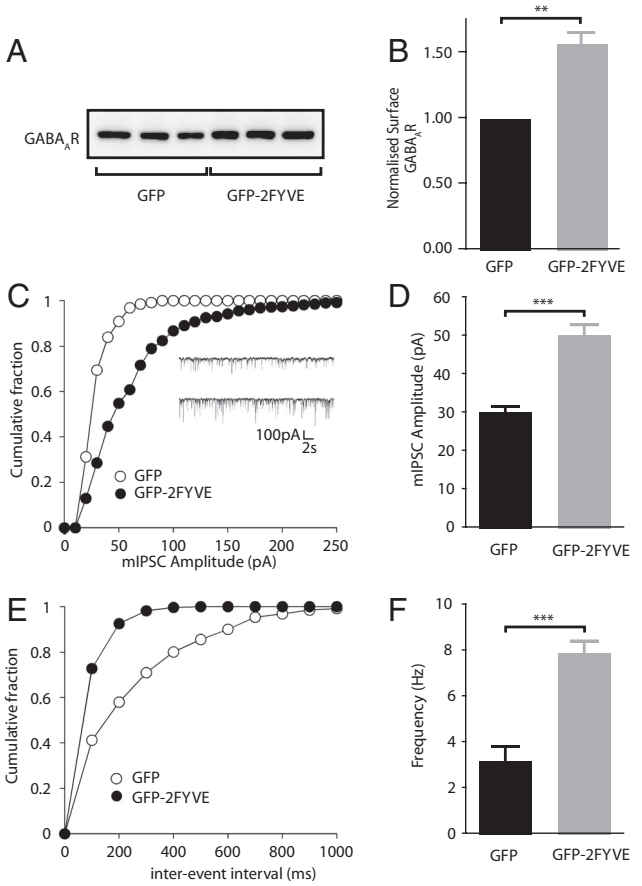

Fig. 3. Functional effects of expressing GFP-2FYVE. (*A*) Cell surface biotinylations of cortical cells expressing GFP or GFP-2FYVE. (*B*) Bar plot summary showing GABA$_A$R surface levels in cells expressing GFP or GFP-2FYVE. Levels are represented as percentage-normalized to those observed in GFP control (n = 11 independent experiments, ***, $P < 0.001$ paired t test). (*C*) Representative cumulative plots and traces (*Inset*) of mIPSC amplitude of representative cells expressing GFP (open circles) or GFP-2FYVE (closed circles). (*D*) Bar plot summary showing the effect of GFP-2FYVE expression on mIPSC amplitude (n = 8–9, ***, $P < 0.001$). (*E*) Representative cumulative plots of mIPSC inter-event interval of representative cells expressing GFP (open circles) or GFP-2FYVE (closed circles). (*F*) Bar plot summary showing the effect of GFP-2FYVE expression on mIPSC frequency (n = 8–9, ***, $P < 0.001$).

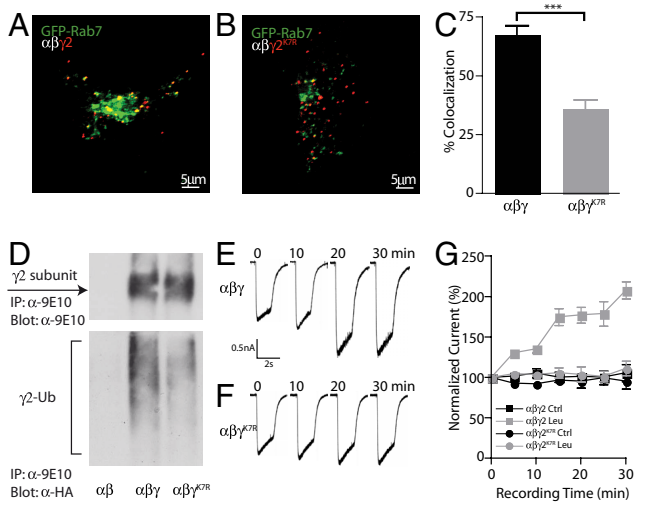

Fig. 4. GABA$_A$R ubiquitination is required for late endosomal/lysosomal targeting. (*A* and *B*) Representative images of internalized $\alpha1\beta3\gamma2$ (*A*) or $\alpha1\beta3\gamma2^{K7R}$ (*B*) in HEK293 cells coexpressing the late endosomal/lysosomal marker GFP-Rab7. (*C*) Summary data of the colocalization levels of internalized GABA$_A$Rs and GFP-Rab7. (*D*) The $\gamma2^{K7R}$ subunit mutant shows decreased levels of ubiquitination compared with the wild-type $\gamma2$ GABA$_A$R subunit. (*E* and *F*) Typical traces of evoked GABAergic currents in HEK-293 cells expressing receptors composed of $\alpha1\beta3\gamma2$ or $\alpha1\beta3\gamma2^{K7R}$ clamped at −70 mV and treated with 20 μM Leupeptin. (*G*) The magnitude of I_{GABA} measured at 5-min intervals was then normalized to that evident at time 0 (5 min after break-in) for cells expressing $\alpha1\beta3\gamma2$ or $\alpha1\beta3\gamma2^{K7R}$ receptors under control conditions and leupeptin treatment (n = 7–11 cells).

colocalization with GFP-Rab7 fluorescence ($\alpha\beta\gamma2$: 67.7 ± 3.8%; $\alpha\beta\gamma2^{K7R}$: 36.3 ± 3.5%) (Fig. 4 *A–C*).

In addition to comparing the lysosomal targeting of GABA$_A$Rs we examined the effects of blocking lysosomal degradation on their functional expression using patch clamp recordings from transfected HEK-293 cells (17, 32). To modulate lysosomal degradation we introduced leupeptin into expressing cells via intracellular dialysis with the patch-pipette. The magnitude of GABA activated membrane currents (I_{GABA}) induced by 5 μM GABA (EC_{50}) (17, 32) were analyzed over a time course of 30 min and normalized to that evident at time 0. In cells expressing receptors incorporating $\gamma2$ subunits leupeptin induced a significant increase in I_{GABA}, which at 30 min reached 207.8 ± 10.6% of that seen at zero time (Fig. 4 *E* and *G*). In contrast in cells expressing $\gamma2^{K7R}$ potentiation of I_{GABA} by leupeptin was insignificant (111.3 ± 8.9%) (Fig. 4 *F* and *G*). In agreement with our imaging studies, leupeptin did not significantly alter I_{GABA} for cells expressing receptors composed of $\alpha\beta$ subunits (107.0 ± 10.4%) (Fig. S4). Therefore, our observations suggest that multiple lysine residues between amino acids 318–337 within the intracellular domain of the $\gamma2$ subunit play a critical role in regulating the late endosomal/lysosomal trafficking of GABA$_A$Rs.

Enhanced Lysosomal Targeting Underlies the Deficits of GABA$_A$R Cell Surface Expression After Anoxia. Protein ubiquitination is increased in the brain upon ischemic injury (33). In addition, several studies have reported compromised synaptic inhibition and a reduction in cell surface GABA$_A$R expression during ischemia (4, 7, 8). Although the cellular mechanisms responsible for this pathological loss of GABA$_A$R functional expression remain unknown, one possible explanation is altered receptor trafficking (4). Therefore, we assessed whether ubiquitin dependent trafficking of GABA$_A$Rs plays a role in the deficit of GABA$_A$R surface expression after ischemia. To examine this, we imaged cultured hippocampal neurons transfected with either $^{GFP}\gamma2$ or $^{GFP}\gamma2^{K7R}$ under control conditions or during oxygen and glucose deprivation (OGD) to induce anoxia. We first investigated whether $^{GFP}\gamma2$ and $^{GFP}\gamma2^{K7R}$ were equally targeted to synaptic sites. We found 75.96 ± 4.5% of GABA$_A$Rs clusters expressing $^{GFP}\gamma2$ and 79.07 ± 2.8% of GABA$_A$Rs expressing $^{GFP}\gamma2^{K7R}$ were found apposed to VIAAT labeled presynaptic inhibitory terminals (Fig. S5). Having established that both $^{GFP}\gamma2$ and $^{GFP}\gamma2^{K7R}$ constructs were equally targeted to synaptic sites, we imaged the fluorescence of individual GFP clusters over time in 12–16DIV cultured hippocampal cells under control and OGD conditions. Analysis of $^{GFP}\gamma2$ subunit containing clusters revealed a significant loss in cluster fluorescence over time under OGD conditions compared with control (OGD t = 30 min: 31.1 ± 2.8%; control t = 30 min: 6.8 ± 5.7%; $P < 0.001$, n = 7–8) (Fig. 5 *A*, *C*, and *D*, and Fig. S6). In contrast, cells expressing $^{GFP}\gamma2^{K7R}$ did not exhibit a significant loss of cluster fluorescence during OGD treatment (OGD t = 30 min: 6.43 ± 6.6%; control t = 30 min: 13.29 ± 3.0%; $P > 0.05$, n = 7–8) (Fig. 5 *B–D* and Fig. S6). Thus, ubiquitin-dependent lysosomal targeting of GABA$_A$Rs results in the loss of synaptic GABA$_A$Rs during OGD treatment. In accordance with these results, the reduction in GABA$_A$R cluster fluorescence observed during OGD was also blocked by leupeptin treatment (Fig. S7). These results provide evidence that modified ubiquitin dependent trafficking of

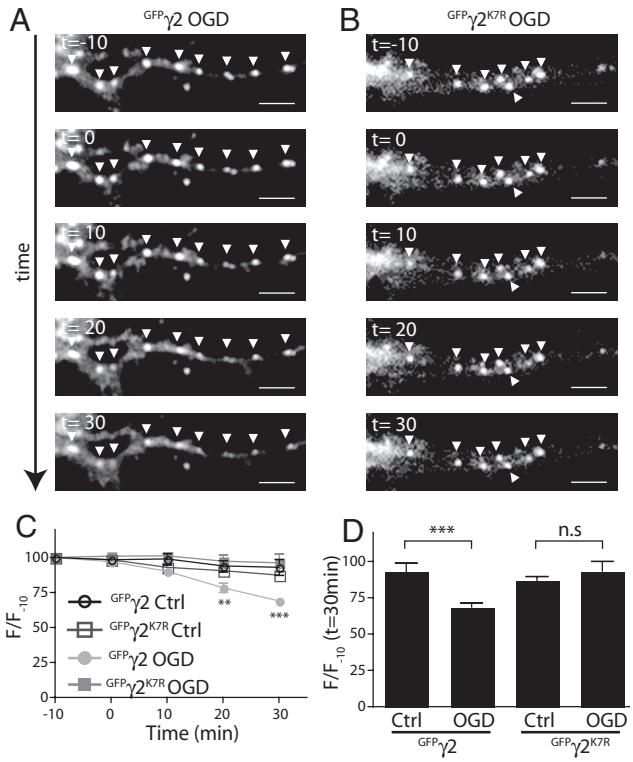

Fig. 5. Oxygen glucose deprivation results in a ubiquitination dependent decrease in $GABA_AR$ surface levels. (*A* and *B*) 25-μm dendritic segment of 12–16 DIV hippocampal cells expressing GFP-tagged $\gamma2$ (*A*) and $\gamma2^{K7R}$ (*B*) imaged over time under OGD conditions. Arrowheads point to GFP clusters. (Scale bar: 5 μm.) (*C*) GFP cluster fluorescence was monitored over time and normalized to $t = -10$ min. (*D*) Summary data plot of normalized cluster fluorescence (F/F_{-10}) at t = 30 min for cells expressing $^{GFP}\gamma2$ and $^{GFP}\gamma2^{K7R}$ (n = 7–8, ***, $P < 0.001$).

$GABA_AR$s in the endocytic pathway may underlie deficits in receptor cell surface stability after ischemia.

Discussion

The regulated endocytosis of ligand-gated ion channels is an important determinant for the efficacy of synaptic transmission (34, 35). Within the endocytic pathway these proteins are recycled or targeted for lysosomal degradation and the impact of this endocytic sorting decision is emerging as an important determinant for neuronal excitability (11, 36). Here, we investigated the role of regulated endocytic sorting with reference to $GABA_AR$s, the principal sites of fast synaptic inhibition in the brain. We demonstrate that acute inhibition of lysosomal activity increases inhibitory synaptic strength by blocking synaptic $GABA_AR$ degradation. In addition, we find that ubiquitination of a motif within the $\gamma2$ subunit is responsible for $GABA_AR$ lysosomal targeting. Furthermore, our results suggest that enhanced ubiquitination dependent degradation of $GABA_AR$s may directly contribute to the previously reported reduction in the number of synaptic $GABA_AR$s observed in ischemia.

The $GABA_AR$ $\gamma2$ subunit confers important pharmacological, functional, and membrane trafficking properties to $GABA_AR$s including the selective targeting of $GABA_AR$s to inhibitory postsynaptic domains (22). In this study, we compared the endocytic fate of $GABA_AR$s composed of $\alpha\beta$ and $\alpha\beta\gamma2$ subunits and found that the $\gamma2$ subunit also plays a key role in the endocytic sorting of $GABA_AR$s, by facilitating the trafficking of $GABA_AR$s to late endocytic/lysosomal compartments. This may provide a mechanism by which neurons can specifically regulate the endocytic trafficking of synaptic ($\gamma2$ subunit containing) $GABA_AR$s without altering the trafficking of other $GABA_AR$s (lacking $\gamma2$ subunits), which may contribute to tonic inhibition.

Using $\beta3/\gamma2$ subunit chimeras we found that a motif within the $\gamma2$ subunit was critically important for the enhanced lysosomal targeting of $GABA_AR$s. This motif was found to be a direct target for ubiquitination and mutation of seven lysine residues within this motif resulted in reduced levels of $GABA_AR$ ubiquitination and compromised targeting to lysosomes. Therefore, these experiments provide compelling evidence that the lysosomal targeting of $GABA_AR$s depends on the ubiquitination of lysine residues between residues 317–338 of the $\gamma2$ subunit. Ubiquitination of lysine residues within the intracellular loops of the $GABA_AR$ $\alpha1$ and $\beta3$ subunits can target unassembled subunits within the endoplasmic reticulum (ER) for ER associated degradation by the proteosome, but does not appear to be involved in $GABA_AR$ endocytic trafficking (17, 18). Moreover, this proteosomal degradation of $GABA_AR$ subunits within the secretory pathway regulates synaptic inhibition over long time scales (days) (17). In contrast, results in this study reveal a mechanism for more rapid (tens of minutes), $\gamma2$ subunit-specific, ubiquitination of $GABA_AR$s resulting in fast regulation of synaptic inhibition.

We found that blocking lysosomal degradation of $GABA_AR$s (with leupeptin treatment) or their ubiquitin-dependent lysosomal targeting (using the dominant negative GFP-2FYVE), caused a marked increase in both mIPSC amplitude and frequency suggesting not only an increase in the number of synaptic $GABA_AR$s but also an increase in the number of synaptic responses. In agreement with these findings, correlative immunofluorescence experiments revealed that blocking lysosomal $GABA_AR$ degradation resulted in an increase both in $GABA_AR$ cluster size and in the number of $GABA_AR$ clusters apposed to VIAAT positive inhibitory presynaptic terminals. The mIPSC amplitude and frequency increase is similar to that observed when surface $GABA_AR$ numbers are increased by dialysing inhibitors of $GABA_AR$ endocytosis into the postsynaptic neuron via the electrophysiological recording pipette (9). We previously suggested that this mIPSC frequency increase reflects the increase in surface $GABA_AR$ number and mIPSC amplitude unmasking mIPSCs that were previously below the threshold for detection in the recordings rather than because of a presynaptic change (9). The changes in $GABA_AR$ cluster number and mIPSC frequency that we report here are similarly likely to be because of the improved detection of existing established synapses (which before blockade of lysosomal targeting contained too few $GABA_AR$s to be detected) as a result of an increase in the availability of surface $GABA_AR$s rather than because of presynaptic effects such as increases in the probability of release.

Modified membrane trafficking of $GABA_AR$s is strongly implicated in a reduction in the number of surface and synaptic $GABA_AR$s, which contributes to the loss of inhibition in status epilepticus (6, 37–39) and ischemic brain injury (4, 8), but the mechanisms have remained unclear. Here, we demonstrate that although anoxic insult reduces the number of wild type GFP-tagged synaptic $GABA_AR$s, the synaptic expression of $GABA_AR$s incorporating $^{GFP}\gamma2^{K7R}$ subunits (and hence no longer ubiquitinated) remained unaffected. Thus, our results suggest that ubiquitin-dependent degradation of $GABA_AR$s may be a key mechanism that underlies the downmodulation of synaptic inhibition after a pathological insult.

In summary, the lysosomal targeting of $GABA_AR$s is modulated by the ubiquitination of lysine residues between amino acids 317–328 within the intracellular domain of the $\gamma2$ subunit. This process regulates the accumulation of $GABA_AR$s at inhibitory synapses and the efficacy of neuronal inhibition under basal conditions, and is responsible for deficits in neuronal inhibition after anoxia.

Materials and Methods

Antibodies and Constructs. For details see *SI Materials and Methods*.

Cell Culture and Transfections. Rat hippocampal and cortical neurons were prepared from embryonic day 18 rat brains. All cell types were transfected by nucleofection as described in ref. 10. See *SI Materials and Methods*.

Brain Slice Preparation and Leupeptin Treatment. Two hundred micrometers frontal cortex coronal sections were prepared from P21 rats and incubated for 3 h in ACSF (126 mM NaCl, 24 mM $NaHCO_3$, 1 mM NaH_2PO_4, 2.5 mM KCl, 1 mM $MgCl_2$, 2 mM $CaCl_2$, 10 mM glucose, and gassed with 95% O_2/5% CO_2) or ACSF supplemented with 200 μM Leupeptin. After treatment, slices were immediately fixed and stained based on protocols from (40, 41). See *SI Materials and Methods*.

Immunofluorescence and Confocal Microscopy. For receptor internalization assays receptors were labeled live with 9E10 anti-myc antibody at 4 °C. Labeled receptors were allowed to internalize for 1 h at 37 °C. Surface antibody was stripped away using 0.2 M acetic acid, 0.5 M NaCl before fixation as described in ref. 34. Internalized receptors were identified using Alexa-fluor594 conjugated goat anti-mouse antibody and confocal microscopy. See *SI Materials and Methods*.

Image Processing and Quantitation. Captured confocal images were analyzed using Metamorph software (Universal Imaging Corporation). See *SI Materials and Methods*.

Live Cell Imaging and Oxygen/Glucose Deprivation. Transfected 12–15DIV hippocampal cultures were imaged in ACSF under constant perfusion (at a rate of 1.3 mL/min). For OGD treatment ACSF was replaced with OGD buffer (126 mM NaCl, 24 mM $NaHCO_3$, 1 mM NaH_2PO_4, 2.5 mM KCl, 1 mM $MgCl_2$, 2 mM $CaCl_2$, 7 mM sucrose, and gassed with 95% N_2/5% CO_2) (42). Images were captured every 10 min for a total of 30 min and analyzed using ImageJ software. See *SI Materials and Methods*.

Biotinylation and Ubiquitination Assays. Cell surface biotinylations were carried out in triplicate on 12–16 DIV cortical cells, as previously described. For ubiquitination assays, Myc-tagged $GABA_A$Rs were immunoprecipitated from transfected HEK cells, as previously described. Precipitates were resolved by SDS/PAGE electrophoresis and analyzed by Western blotting. See *SI Materials and Methods*.

Electrophysiology. Whole-cell recordings of mIPSCs from cortical slices, or GFP-2FYVE transfected cultured cortical cells, were performed using standard voltage clamp techniques in the presence of CNQX (20 μM) and APV (40 μM) to block AMPA and NMDA receptors, respectively (43, 44). Membrane currents from HEK-293 cells were measured, as outlined previously at 32 °C (10, 43, 45). Data were collected 5 min after obtaining a stable recording conformation. See *SI Materials and Methods*.

ACKNOWLEDGMENTS. S.J.M. was supported by NINDS grants NS047478, NS048045, NS051195, NS056359, and NS054900, and R.S.S. was supported by a fellowship from the American Scoiety for Epilepsy. J.T.K. was supported by the MRC, UK.

1. Jacob TC, Moss SJ, Jurd R (2008) GABA(A) receptor trafficking and its role in the dynamic modulation of neuronal inhibition. *Nat Rev Neurosci* 9:331–343.
2. Nusser Z, Cull-Candy S, Farrant M (1997) Differences in synaptic GABA(A) receptor number underlie variation in GABA mini amplitude. *Neuron* 19:697–709.
3. Arancibia-Carcamo IL, Kittler JT (2009) Regulation of GABA(A) receptor membrane trafficking and synaptic localization. *Pharmacol Ther* 123:17–31.
4. Mielke JG, Wang YT (2005) Insulin exerts neuroprotection by counteracting the decrease in cell-surface GABA receptors after oxygen-glucose deprivation in cultured cortical neurons. *J Neurochem* 92:103–113.
5. Kang JQ, Shen W, Macdonald RL (2006) Why does fever trigger febrile seizures? GABAA receptor gamma2 subunit mutations associated with idiopathic generalized epilepsies have temperature-dependent trafficking deficiencies. *J Neurosci* 26:2590–2597.
6. Naylor DE, Liu H, Wasterlain CG (2005) Trafficking of GABA(A) receptors, loss of inhibition, and a mechanism for pharmacoresistance in status epilepticus. *J Neurosci* 25:7724–7733.
7. Zhan RZ, Nadler JV, Schwartz-Bloom RD (2006) Depressed responses to applied and synaptically-released GABA in CA1 pyramidal cells, but not in CA1 interneurons, after transient forebrain ischemia. *J Cereb Blood Flow Metab* 26:112–124.
8. Schwartz-Bloom RD, Sah R (2001) Gamma-Aminobutyric acid(A) neurotransmission and cerebral ischemia. *J Neurochem* 77:353–371.
9. Kittler JT, et al. (2000) Constitutive endocytosis of GABAA receptors by an association with the adaptin AP2 complex modulates inhibitory synaptic currents in hippocampal neurons. *J Neurosci* 20:7972–7977.
10. Kittler JT, et al. (2004) Huntingtin-associated protein 1 regulates inhibitory synaptic transmission by modulating gamma-aminobutyric acid type A receptor membrane trafficking. *Proc Natl Acad Sci USA* 101:12736–12741.
11. Park M, Penick EC, Edwards JG, Kauer JA, Ehlers MD (2004) Recycling endosomes supply AMPA receptors for LTP. *Science* 305:1972–1975.
12. Hicke L, Dunn R (2003) Regulation of membrane protein transport by ubiquitin and ubiquitin-binding proteins. *Annu Rev Cell Dev Biol* 19:141–172.
13. Martin S, Nishimune A, Mellor JR, Henley JM (2007) SUMOylation regulates kainate-receptor-mediated synaptic transmission. *Nature* 447:321–325.
14. Patrick GN (2006) Synapse formation and plasticity: Recent insights from the perspective of the ubiquitin proteasome system. *Curr Opin Neurobiol* 16:90–94.
15. Yi JJ, Ehlers MD (2007) Emerging roles for ubiquitin and protein degradation in neuronal function. *Pharmacol Rev* 59:14–39.
16. Segref A, Hoppe T (2009) Think locally: Control of ubiquitin-dependent protein degradation in neurons. *EMBO Rep* 10:44–50.
17. Saliba RS, Michels G, Jacob TC, Pangalos MN, Moss SJ (2007) Activity-dependent ubiquitination of GABA(A) receptors regulates their accumulation at synaptic sites. *J Neurosci* 27:13341–13351.
18. Gallagher MJ, Ding L, Maheshwari A, Macdonald RL (2007) The GABAA receptor alpha1 subunit epilepsy mutation A322D inhibits transmembrane helix formation and causes proteasomal degradation. *Proc Natl Acad Sci USA* 104:12999–13004.
19. Haglund K, Di Fiore PP, Dikic I (2003) Distinct monoubiquitin signals in receptor endocytosis. *Trends Biochem Sci* 28:598–603.
20. Raiborg C, Rusten TE, Stenmark H (2003) Protein sorting into multivesicular endosomes. *Curr Opin Cell Biol* 15:446–455.
21. Dumoulin A, et al. (1999) Presence of the vesicular inhibitory amino acid transporter in GABAergic and glycinergic synaptic terminal boutons. *J Cell Sci* 112:811–823.
22. Essrich C, Lorez M, Benson JA, Fritschy JM, Luscher B (1998) Postsynaptic clustering of major GABAA receptor subtypes requires the gamma 2 subunit and gephyrin. *Nat Neurosci* 1:563–571.
23. Crestani F, et al. (1999) Decreased GABAA-receptor clustering results in enhanced anxiety and a bias for threat cues. *Nat Neurosci* 2:833–839.
24. Connolly CN, et al. (1999) Cell surface stability of gamma-aminobutyric acid type A receptors. Dependence on protein kinase C activity and subunit composition. *J Biol Chem* 274:36565–36572.
25. Kittler JT, et al. (2008) Regulation of synaptic inhibition by phospho-dependent binding of the AP2 complex to a YECL motif in the GABAA receptor gamma2 subunit. *Proc Natl Acad Sci USA* 105:3616–3621.
26. Bucci C, Thomsen P, Nicoziani P, McCarthy J, van Deurs B (2000) Rab7: A key to lysosome biogenesis. *Mol Biol Cell* 11:467–480.
27. Meresse S, Gorvel JP, Chavrier P (1995) The rab7 GTPase resides on a vesicular compartment connected to lysosomes. *J Cell Sci* 108:3349–3358.
28. Wooltorton JR, Moss SJ, Smart TG (1997) Pharmacological and physiological characterization of murine homomeric beta3 GABA(A) receptors. *Eur J Neurosci* 9:2225–2235.
29. Taylor PM, et al. (1999) Identification of amino acid residues within GABA(A) receptor beta subunits that mediate both homomeric and heteromeric receptor expression. *J Neurosci* 19:6360–6371.
30. Williams RL, Urbe S (2007) The emerging shape of the ESCRT machinery. *Nat Rev Mol Cell Biol* 8:355–368.
31. Petiot A, Faure J, Stenmark H, Gruenberg J (2003) PI3P signaling regulates receptor sorting but not transport in the endosomal pathway. *J Cell Biol* 162:971–979.
32. Bogdanov Y, et al. (2006) Synaptic GABAA receptors are directly recruited from their extrasynaptic counterparts. *EMBO J* 25:4381–4389.
33. Hu BR, Martone ME, Jones YZ, Liu CL (2000) Protein aggregation after transient cerebral ischemia. *J Neurosci* 20:3191–3199.
34. Carroll RC, Beattie EC, von Zastrow M, Malenka RC (2001) Role of AMPA receptor endocytosis in synaptic plasticity. *Nat Rev Neurosci* 2:315–324.
35. Groc L, Choquet D (2006) AMPA and NMDA glutamate receptor trafficking: Multiple roads for reaching and leaving the synapse. *Cell Tissue Res* 326:423–438.
36. Park M, et al. (2006) Plasticity-induced growth of dendritic spines by exocytic trafficking from recycling endosomes. *Neuron* 52:817–830.
37. Terunuma M, et al. (2008) Deficits in phosphorylation of GABA(A) receptors by intimately associated protein kinase C activity underlie compromised synaptic inhibition during status epilepticus. *J Neurosci* 28:376–384.
38. Goodkin HP, Yeh JL, Kapur J (2005) Status epilepticus increases the intracellular accumulation of GABAA receptors. *J Neurosci* 25:5511–5520.
39. Goodkin HP, Joshi S, Mtchedlishvili Z, Brar J, Kapur J (2008) Subunit-specific trafficking of GABA(A) receptors during status epilepticus. *J Neurosci* 28:2527–2538.
40. Schneider Gasser EM, et al. (2006) Immunofluorescence in brain sections: Simultaneous detection of presynaptic and postsynaptic proteins in identified neurons. *Nat Protoc* 1:1887–1897.
41. Karadottir R, Attwell D (2006) Combining patch-clamping of cells in brain slices with immunocytochemical labeling to define cell type and developmental stage. *Nat Protoc* 1:1977–1986.
42. Allen NJ, Rossi DJ, Attwell D (2004) Sequential release of GABA by exocytosis and reversed uptake leads to neuronal swelling in simulated ischemia of hippocampal slices. *J Neurosci* 24:3837–3849.
43. Kittler JT, et al. (2005) Phospho-dependent binding of the clathrin AP2 adaptor complex to GABAA receptors regulates the efficacy of inhibitory synaptic transmission. *Proc Natl Acad Sci USA* 102:14871–14876.
44. Chen G, Kittler JT, Moss SJ, Yan Z (2006) Dopamine D3 receptors regulate GABAA receptor function through a phospho-dependent endocytosis mechanism in nucleus accumbens. *J Neurosci* 26:2513–2521.
45. Jacob TC, et al. (2005) Gephyrin regulates the cell surface dynamics of synaptic GABAA receptors. *J Neurosci* 25:10469–10478.